Available online at www.sciencedirect.com
ScienceDirect
Journal of the European Ceramic Society 28 (2008) 787–792
www.elsevier.com/locate/jeurceramsoc

The preparation and mechanical properties of the unidirectional carbon fiber reinforced zirconia composite

G.H. Zhou [a,b], S.W. Wang [a,*], J.K. Guo [a], Z. Zhang [a]

[a] *Shanghai Institute of Ceramics, Chinese Academy of Sciences, 1295 Dingxi Road, Shanghai 200050, PR China*
[b] *Graduate School of Chinese Academy of Sciences, Beijing 100049, PR China*

Received 14 March 2007; received in revised form 25 June 2007; accepted 6 July 2007
Available online 14 September 2007

Abstract

Unidirectional carbon fiber reinforced calcium stabilized zirconia composites (uni-C_f/ZrO_2) were prepared by slurry infiltration and hot-pressing method. The room temperature mechanical properties were investigated and the fracture features of composites were observed. A flexural strength of 588.0 MPa and fracture toughness of 15.4 MPa·$m^{1/2}$ parallel to the fiber direction for the composite hot-pressed at 1500 °C was attributed to the fiber pull-out. With increasing hot-pressing temperature from 1500 °C to 1650 °C, the relative density was augmented, but the mechanical properties of composites degraded gradually. Especially at 1650 °C, the flexural strength and fracture toughness decreased significantly to 173.2 MPa and 5.0 MPa·$m^{1/2}$, respectively. Thermodynamic calculation and XRD, TEM investigations showed that carbon fibers reacted with ZrO_2 to form ZrC phase at 1650 °C, and then formed chemical bonding and led to a strong interface between fiber and matrix, which resulted in the decrease of mechanical properties of the composite hot-pressed at higher temperatures. Moreover, the mechanical properties of carbon fibers degraded by the above reaction had also an adverse effect on the mechanical properties of the composite.

Keywords: Hot-pressing; Composites; Mechanical properties; ZrO_2; Carbon fiber

1. Introduction

Zirconia-based composites have demonstrated a wide range of attributes, including high melting point ($T_m \approx 2700$ °C) and stability, high strength and toughness, good heat resistance, unique wear resistance, interesting electronic properties such as fast ionic conductivity for structural and functional applications.[1,2] As well known, the problem of the low fracture toughness of ceramics can be overcome by designing and preparing composite materials reinforced with fibers, whiskers and particles. Up to now, surprisingly there are a few researches on ZrO_2–matrix composites reinforced with continuous fibers. Pujari and Jawed[3] reported chopped alumina fiber–TZP matrix composites prepared by a conventional powder metallurgy route. They found that the alumina fibers did result in a twofold increase in toughness with respect to the monolithic TZP but the failure mode remained brittle. In the meantime, Bender et al.[4] succeeded in preparing ZrO_2–SiO_2 and ZrO_2–TiO_2 matrix composites reinforced with uncoated or BN coated SiC fibers according to a liquid route (organometallic precursors). Their composites exhibited brittle failure when reinforced with uncoated SiC fibers due to a strong fiber–matrix bonding whereas they did behave in a non-brittle manner with BN-coated SiC fibers, the BN layer allowing the fiber pull-out to occur and preventing the fibers reacting with the matrix. Subsequently, Minet et al.[5] prepared ZrO_2-based composites by CVI densification from performs made of alumina and carbon fibers consolidated with a small amount of alumina, pyrocarbon or hex-BN. The composites mechanical properties exhibited similar to those already reported for the related C/SiC, C/B_4C, C/TiC or C/BN materials. Compared with the CVI procedure, the traditional slurry infiltration and hot-pressing method has some advantages such as low cost, short processing time and higher densification.

The aim of present work was to explore the potential of continuous carbon fibers reinforced zirconia-based composites (C_f/ZrO_2) for aerospace applications. Unidirectional carbon fibers reinforced zirconia composite was prepared by

* Corresponding author. Tel.: +86 21 52414320; fax: +86 21 52415263.
E-mail address: swwang51@mail.sic.ac.cn (S.W. Wang).

0955-2219/$ – see front matter © 2007 Elsevier Ltd. All rights reserved.
doi:10.1016/j.jeurceramsoc.2007.07.005

Table 1
The mechanical properties of ZrO_2 and C_f/ZrO_2 composite

	Temperature (°C)	Relative density (%)	Flexural strength (MPa)	Elastic modulus (GPa)	K_{IC} (MPa·m$^{1/2}$)
ZrO_2	1500	98.8	125.8 ± 12.1	117.3 ± 4.3	3.2 ± 0.1
C_f/ZrO_2	1500	95.4	588.0 ± 71.8	94.7 ± 1.5	15.4 ± 0.8
	1550	96.6	547.4 ± 38.8	90.3 ± 2.5	14.2 ± 1.1
	1600	96.8	508.3 ± 18.4	86.7 ± 3.2	12.3 ± 1.6
	1650	98.5	173.2 ± 2.0	75.0 ± 3.5	5.0 ± 0.3

slurry infiltration and hot-pressing sintering method. The effect of hot-pressing temperature on the mechanical properties of composite was investigated. The morphologies of composite fracture surface were observed. Transmission electronic microscope examined the microstructural features of fiber/matrix interface.

2. Experimental procedures

ZrO_2 powder (containing 6.6 wt.% CaO, ZrO_2 > 93 wt.% and average particle size around 2 μm), and PAN-based carbon fibers (4800 MPa average tensile strength, and 5 μm in diameter), were used as starting materials. The powders were mixed in deionized water with carboxymethyl cellulose (CMC) as a binder and *iso*-propyl alcohol as a dispersant, and then ball-milled with agate balls. The prepreg was prepared by infiltrating the continuous carbon fibers into the slurry and then dried, stacked in a graphite die and hot-pressed between 1500 and 1650 °C and 25 MPa in a Ar atmosphere. The content of carbon fiber was approximately 30 vol.% in the composites. For comparison, hot-pressed ZrO_2 specimen without reinforcement was also prepared.

Density measurements were performed based on Archimedes principle. The specimens were machined into bars of 36 mm × 4 mm × 3 mm parallel to the fiber direction to measure the flexural strength by the three-point bending method with a span of 30 mm and a cross-head speed of 0.5 mm/min, at room temperature in air. Single-edge notched-beam (SENB) samples were fabricated by notching the segments of tested flexure specimens with a 0.20 mm thick diamond wafering saw. The 30 mm × 6 mm × 3 mm SENB samples were tested in three-point loading with a span of 24 mm and a cross-head speed of 0.05 mm/min. Fracture toughness K_{IC} was calculated by the ASTME 399-74 formula.[6] The flexural strength and the fracture toughness measurements were conducted by Instron-5566 testing machine. Five specimens were tested for each sample.

Flexural strength was calculated by the following equation[7]:

$$\sigma_f = \frac{3PL}{2bd^2} \quad (1)$$

where σ_f is the flexural strength (maximum stress at mid-span), P the applied load that leads the specimen to fail, L the support span, b the specimen width and, finally d is the specimen thickness.

Effective engineering modulus was obtained from the slope of the initial straight-line of the load–displacement curve by means of this equation[8]:

$$E = \frac{L^3}{48I}\frac{F}{\delta} \quad (2)$$

where F/δ represents the slope of the load–displacement curve and I is the cross-sectional inertia of the specimen.

The phase compositions of the samples were examined by X-ray diffractometer (D/max 2550 V). The fracture surfaces of the specimens were observed by scanning electronic microscope (SEM, Model JXA-8100, Jeol Co., Tokyo, Japan). The microstructural features of fiber/matrix interface were characterized using transmission electronic microscope (TEM, Model 200CX, Jeol, Japan).

3. Results and discussion

Table 1 lists the mechanical properties of ZrO_2 and C_f/ZrO_2 composite. When hot pressed at 1500 °C, it can be seen that flexural strength and fracture toughness are 125.8 MPa and 3.2 MPa·m$^{1/2}$, respectively, for ZrO_2 without the reinforcement of carbon fiber. While, flexural strength and fracture toughness of the composites were 588.0 MPa and 15.4 MPa·m$^{1/2}$, respectively, which were the five-fold that of ZrO_2. On the other hand, with the increase of the hot-pressing temperature from 1500 °C to 1650 °C, the mechanical properties decreased gradually though the relative density of the composite increased. For the composite hot-pressed at 1650 °C, the flexural strength and fracture toughness decreased sharply to 173.2 MPa and 5.0 MPa·m$^{1/2}$, respectively.

The typical morphologies of C_f/ZrO_2 composite specimens are shown in Fig. 1. It can be seen that the cracks are zigzag

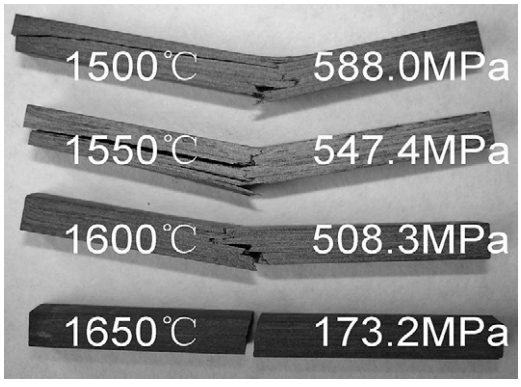

Fig. 1. Typical morphologies of C_f/ZrO_2 composite specimens after flexural test.

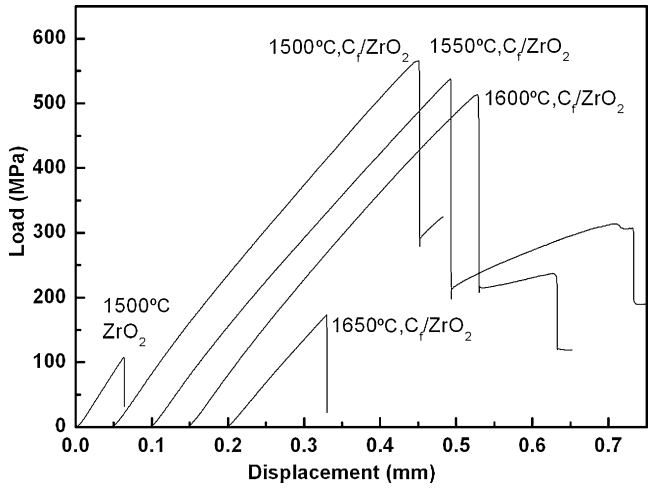

Fig. 2. Load–displacement curves of ZrO_2 and C_f/ZrO_2 composite.

and tend to propagate parallel to the direction of carbon fiber when the samples were hot-pressed at 1500 °C, 1550 °C and 1600 °C. Because of the debonding at the fiber/matrix interface, the matrix crack did not penetrate the fibers, which then remained to bridge the matrix crack and restrained the crack opening. But at 1650 °C, the matrix crack penetrated into the fibers and the fibers were broken, thus the specimen shows brittle fracture behavior.

Fig. 2 shows the typical load–displacement curves of ZrO_2 and C_f/ZrO_2 composites. From Fig. 2, ZrO_2 sample showed elastic loading up to the onset of brittle failure, which is typical fracture mode of most ceramics materials. In contrast, C_f/ZrO_2 composites hot-pressed at 1500 °C, 1550 °C and 1600 °C showed the first elastic response in the initial stages, and then a deviation happened at some load, indicating occurrence of microcracking in the ZrO_2 matrix. After that, the second elastic response appeared up to the maximum load where a significant drop in load occurred, which was attributed to fiber bundle failure near the tensile surface in the three-point bending test. Where after, the final stage was a non-linear region—the tail of curve, revealing fiber pull-out, bridging, and sliding.[9,10] But in the case of the composite hot-pressed at 1650 °C, the load–displacement curve is the same as that of ZrO_2.

Fig. 3 shows fracture surface morphologies of C_f/ZrO_2 composite hot-pressed at different temperatures. For the composites hot-pressed at 1500 °C and 1550 °C, large fiber pull-out was observed on the fracture surface (Fig. 3a and b). It indicated that the reinforcing effect of C_f was significant and the continuous fiber played an important role in carrying the load. Fiber pull-out was also found on the fracture surface of the composite hot-pressed at 1600 °C, however, the pull-out length was far shorter than that of the two specimens mentioned above (Fig. 3c). For 1650 °C, the fracture surface was very flat and no fiber pull-out could be observed (Fig. 3d). These were consistent with the load–displacement curves of C_f/ZrO_2 composites in Fig. 2.

Curtin,[11] Curtin and Zhou[12] and Hui et al.[13] had developed a theory that explained the load–displacement behavior for the ceramic matrix composites (CMCs) as a function of the characteristic matrix strength parameter σ_R. Lower σ_R led to increased matrix cracking and non-linear deformation, and larger failure strains, with both failure stress and failure strain

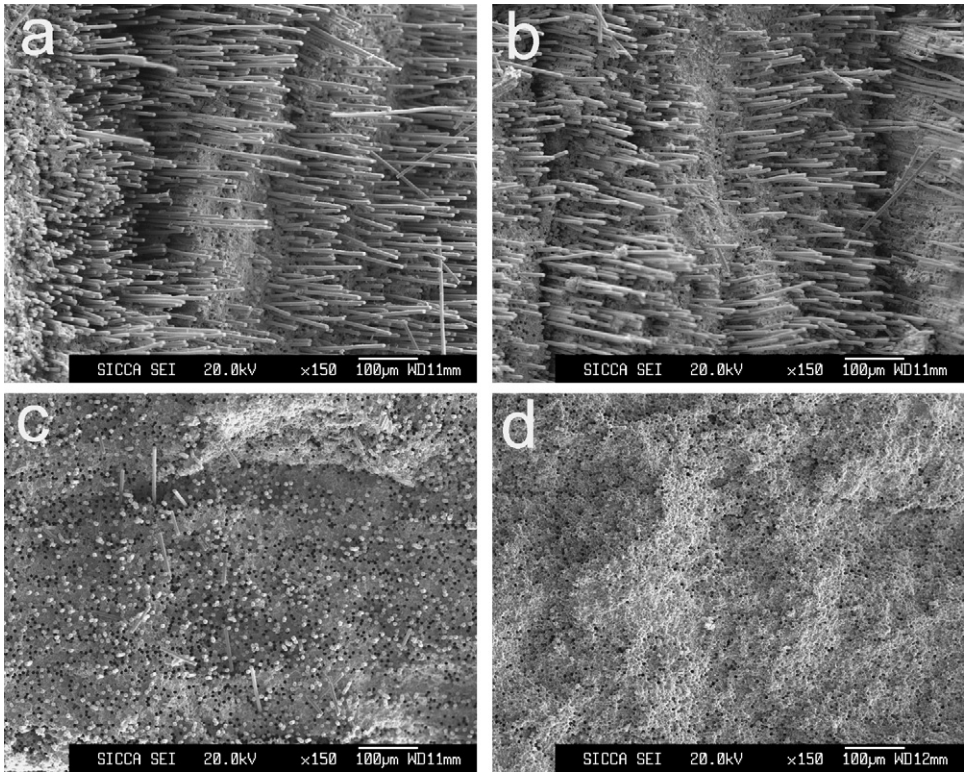

Fig. 3. The morphologies of fracture surface: (a) 1500 °C, (b) 1550 °C, (c) 1600 °C and (d) 1650 °C.

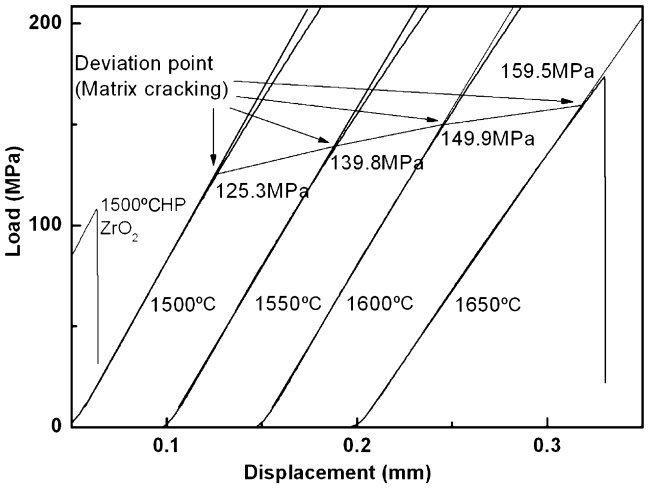

Fig. 4. The first elastic response of the load–displacement curves.

controlled by the fibers, which was referred as "tough" behavior; larger σ_R led to nearly linear deformation and low failure strains controlled by the matrix (brittle), which was referred as "brittle" behavior. Presently, similar cases could be seen from the load–displacement curves given in Fig. 2. Hot-pressed at 1500 °C, 1550 °C and 1600 °C, the C_f/ZrO_2 composite exhibited "tough" behavior, while it was "brittle" behavior when hot-pressed at 1650 °C. Fig. 4 gives the first elastic response of the load–displacement curves. It can be seen that if a beeline is drawn which matches the end of the first elastic response, the deviation point indicating the occurrence of the matrix cracking can be clearly discerned. For the increasing hot-pressing temperature 1500 °C, 1550 °C, 1600 °C and 1650 °C, the deviation point occurs for 125.3 MPa, 139.8 MPa, 149.9 MPa and 159.5 MPa, respectively. That is, the higher hot-pressing temperature, the higher matrix cracking stress, which may be attributed to the improved relative density at higher hot-pressing temperatures. Thus, at 1500 °C, 1550 °C and 1600 °C it belonged to the case of lower σ_R, whereas, at 1650 °C it belonged to the case of larger σ_R.

Fig. 5 shows magnified micrographs of fracture surface of the composite hot-pressed at 1500 °C and 1650 °C. At 1500 °C, it can be seen much matrix cracking at the ZrO_2 grain boundary after the composite failed at the flexural load (Fig. 5a, white arrow). When the matrix cracks propagated and encountered the carbon fiber, they were deflected, so around the carbon fibers cracking also could be seen, which led to debonding at the fiber/matrix interface and fibers easily pulled out from the matrix. But at 1650 °C, little matrix cracking could be seen at the fracture surface (Fig. 5b). It was attributed to the larger matrix strength parameter mentioned above. When the matrix cracking initiated at a higher load, it penetrated into the fiber to propagate and then fibers were broken. It was consistent with the composite failing strength around only a single matrix crack, which was firstly studied by Thouless and Evans.[14,15]

On the other hand, at high hot-pressing temperature the carbon fiber and oxide matrix may happen to react together, which will play a negative role in the mechanical properties of composite. On the basis of the various standard Gibbs free energies of formation listed in Table 2,[16] it can be deduced the Gibbs free

Table 2
The reactions and standard Gibbs free energy

Reaction	Standard Gibbs free energy ($J \cdot mol^{-1}$)
(1) $C_{(s)} + 0.5O_{2(g)} = CO_{(g)}$	$\Delta G^\circ = -114400 - 85.77T$
(2) $Zr_{(s)} + C_{(s)} = ZrC_{(s)}$	$\Delta G^\circ = -196650 + 9.2T$
(3) $Zr_{(s)} + O_{2(g)} = ZrO_{2(s)}$	$\Delta G^\circ = -1092000 + 183.7T$

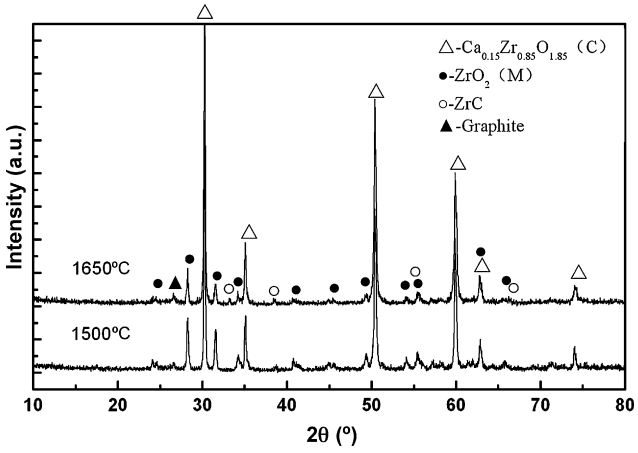

Fig. 6. XRD patterns of the composite at 1500 °C and 1650 °C.

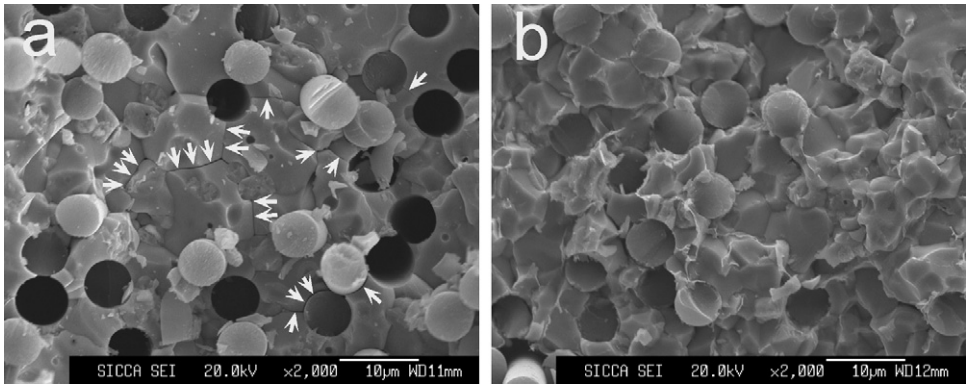

Fig. 5. The magnified micrographs of fracture surface: (a) 1500 °C and (b) 1650 °C.

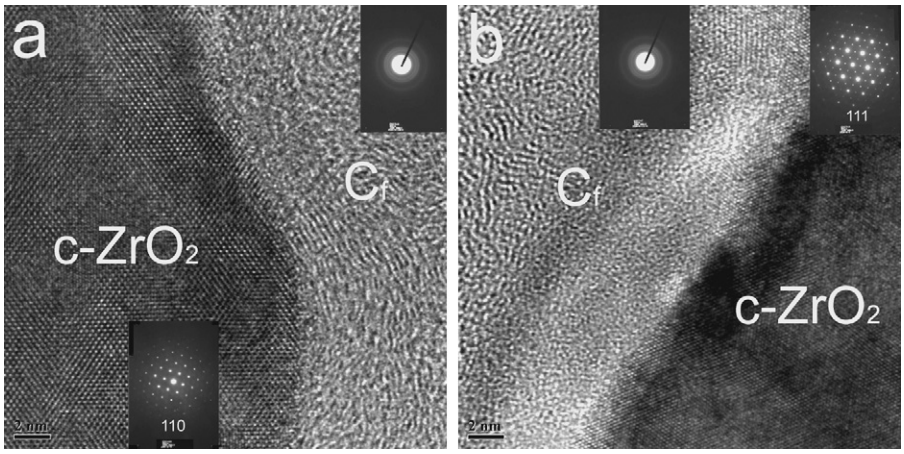

Fig. 7. High-resolution transmission electron micrograph of the composite: (a) 1500 °C and (b) 1650 °C. Inset: selected area electron diffraction pattern.

energy of the following reaction:

$$ZrO_{2(s)} + 3C_{(s)} = ZrC_{(s)} + 2CO_{(g)},$$
$$\Delta G^{\circ} = 666550 - 346.04T \quad (3)$$

If neglect the equilibrium partial pressure of $CO_{(g)}$, reaction (3) could occur on the condition of ΔG° becomes less than zero and correspondingly the T is more than 1653 °C. So in the case of present work, carbon fiber may react with ZrO_2 matrix to form ZrC phase. Fig. 6 gives the XRD patterns of C_f/ZrO_2 composite at 1500 °C and 1650 °C. Hot-pressed at 1500 °C, besides little monoclinic zirconia (m-ZrO_2) and graphite phase, calcium stabilized cubic zirconia ($Ca_{0.15}Zr_{0.85}O_{1.85}$, c-$ZrO_2$, JCPDS PDF no.: 26-0341) is the primary phase in the specimen. But when hot-pressed at 1650 °C, the peak intensity of monoclinic ZrO_2 was weakened and that of $Ca_{0.15}Zr_{0.85}O_{1.85}$ phase was enhanced. It indicated that high hot-pressing temperature was helpful for the conversion of m-ZrO_2 to c-ZrO_2. However, little amount of ZrC phase appeared simultaneously in the products at 1650 °C. All these testified the above speculation and indicated that at higher hot-pressing temperature carbon fiber reacted with ZrO_2 matrix into ZrC phase.

Fig. 7a and b shows high-resolution transmission electron micrograph of C_f/ZrO_2 at 1500 °C and 1650 °C, respectively. From Fig. 7a, it can be seen a clear interface between carbon fiber and matrix at 1500 °C. The selected area electron diffraction pattern indicated cubic zirconia and amorphous carbon. But at 1650 °C, there was an indistinct interlayer at the fiber/matrix interface. Cubic zirconia and carbon fiber can also be distinguished by selected area electron diffraction. However, it failed to explore the ZrC phase at the fiber/matrix interface. In the light of above analysis, when C_f/ZrO_2 composite was hot-pressed at 1650 °C, carbon fiber reacted with ZrO_2 matrix to form ZrC phase, and then chemical bonding formed, which led to a strong interface between fiber and matrix. First, the reaction would degrade the mechanical properties of carbon fiber. This was responsible for the decreased mechanical properties of composite. Secondly, in the light of interface theory of ceramic matrix composites (CMCs), strong fiber/matrix interfacial bonding results in the matrix microcrackings propagating through the fiber with the increase of load. So, with increasing hot-pressing temperature the fiber pull-out length became shorter, especially at 1650 °C where no fiber pull-out was observed and the composite revealed brittle failure behavior.

4. Conclusions

1. Uni-C_f/ZrO_2 composite was prepared by slurry infiltration and hot-pressing. A flexural strength of 588.0 MPa and fracture toughness of 15.4 $MPa \cdot m^{1/2}$ parallel to the fiber direction for the uni-C_f/ZrO_2 composite hot-pressed at 1500 °C was attributed to the fiber pull-out.
2. Different densification of the composite hot-pressed at between 1500 °C and 1650 °C resulted in the different matrix strength parameter. At lower hot-pressing temperature, the lower matrix strength parameter led to increased matrix cracking and non-linear deformation, and larger failure strains, with both failure stress and failure strain controlled by the fibers, so the composite exhibited "toughness" behavior. But for the composite hot-pressed at 1650 °C, the larger matrix strength parameter resulted in the matrix cracking initiated at higher load and nearly linear deformation and low failure strains controlled by the matrix, so the composite showed "brittle" behavior.
3. Thermodynamic calculations and XRD, TEM results showed that carbon fiber reacted with ZrO_2 into ZrC phase at 1650 °C, and then formed chemical bonding and led to a strong interface between fiber and matrix. Moreover, the reaction degraded the mechanical properties of carbon fiber. These were responsible for the decreased mechanical properties of uni-C_f/ZrO_2 composite hot-pressed at higher temperatures.

References

1. Swain, M. V. and Rose, L. R., Strong limitations of transformation-toughened zirconia alloys. *J. Am. Ceram. Soc.*, 1986, **69**, 511.
2. Cesari, F., Esposito, L., Furgiuele, F. M., Maletta, C. and Tucci, A., Fracture toughness of alumina-zirconia composites. *Ceram. Int.*, 2006, **32**, 249–255.
3. Pujari, V. K. and Jawed, I., The alumina fibre/tetragonal zirconia polycrystal composite system. *Composites*, 1986, **17**(2), 137–140.

4. Bender, B., Shadwell, D., Bulik, C., Incorvati, L. and Lewis III, D., Effect of fiber coating and composite processing on properties of zirconia-based matrix SiC fiber composites. *Ceram. Bull.*, 1986, **65**(2), 363–369.
5. Minet, J., Langlais, F., Quenisset, J. M. and Naslain, R., Thermomechanical properties and oxidation resistance of zirconia CVI–matrix composites: 1. Mechanical behavior. *J. Eur. Ceram. Soc.*, 1989, **5**, 341–356.
6. Guan, Z. D., Zhang, Z. T. and Jiao, J. S., *The physical properties of inorganic materials*. Tsinghua University Publishing Company, 1992, p.59.
7. ASTM. Standard test method for flexural properties of unreinforced and reinforced plastics and electrical insulating materials. D790, 1998.
8. Sánchez-Sáez, S., Gómez-del Río, T., Barbero, E. *et al.*, Static behavior of CFRPs at low temperatures. *Compos. B: Eng.*, 2002, **33**, 383–390.
9. Jia, D. C., Zhou, Y. and Lei, T. Q., Ambient and elevated temperature mechanical properties of hot-pressed fused silica matrix composite. *J. Eur. Ceram. Soc.*, 2003, **23**, 801–808.
10. Evans, A. G. and Marshall, D. B., The mechanical performance of fiber reinforced ceramic matrix composites, high temperature/high performance composites. In *Materials Research Society Symposium Proceeding, vol. 120*, ed. F. D. Lemkey and S. G. Fishman *et al.* 1988, pp. 213–246.
11. Curtin, W. A., Theory of mechanical properties of ceramic–matrix composites. *J. Am. Ceram. Soc.*, 1991, **74**, 2837–2845.
12. Curtin, W. A. and Zhou, S. J., Influence of processing damage on performance of fiber-reinforced composites. *J. Mech. Phys. Solids*, 1995, **43**, 343–363.
13. Hui, C. Y., Phoenix, S. L., Ibnabdelialil, M. and Smith, R. L., An exact closed form solution for fragmentation of Weibull fibers in a single filament composite with applications to fiber-reinforced ceramics. *J. Mech. Phys. Solids*, 1995, **43**, 1551–1585.
14. Thouless, M. D. and Evans, A. G., Effects of pull-out on the mechanical properties of ceramic–matrix composites. *Acta Metall.*, 1988, **3**(36), 517–522.
15. Thouless, M. D., Sbaizero, O., Sigl, L. S. and Evans, A. G., Effect of interface mechanical properties on pullout in a sic-fiber-reinforced lithium aluminum silicate glass-ceramic. *J. Am. Ceram. Soc.*, 1989, **72**, 525–532.
16. Liang, Y. J. and Che, M. C., *Handbook of thermodynamics data of inorganic materials*. Northeastern University Publications, Shenyang, 1993.